**One Earth, Volume *7***

## Supplemental information

# Human heat stress could offset potential economic benefits of $CO_2$ fertilization in crop production under a high-emissions scenario

**Anton Orlov, Jonas Jägermeyr, Christoph Müller, Anne Sophie Daloz, Florian Zabel, Sara Minoli, Wenfeng Liu, Tzu-Shun Lin, Atul K. Jain, Christian Folberth, Masashi Okada, Benjamin Poschlod, Andrew Smerald, Julia M. Schneider, and Jana Sillmann**

Supplementary Information

## Contents

## Supplemental Experimental Procedures

### Daily mean vs. hourly responses

Bias-adjusted hourly climate model data is not available. Therefore, we use daily mean values. To test our results for a potential underestimation, we apply the Teddy–tool v1.1 (TEmporal Disaggregation of DailY Climate Model Data) for temporal disaggregation of daily ISIMIP3b climate model data to hourly timeseries [1]. The applied method for disaggregation compares every single day of a given climate model dataset to daily bias-adjusted WFDE5 reanalysis data (1980-2019). For the day of interest at a specific location, the Teddy-Tool identifies the most similar climatic day at the same location within a predefined time window (+/- 5 days) around the day of interest. For the best fit, it applies the historical hourly diurnal profile (based on bias-adjusted hourly WFDE5 reanalysis data) to the climate model daily mean value. Thereby, the Teddy-Tool conserves mass and energy in all cases and strictly preserves the daily mean value (sum for precipitation) of the climate model. The physical relationship between temperature and relative humidity is considered and oversaturation is restricted. For radiation, precalculated potential incoming shortwave radiation is set as a maximum. For temperature, daily maximum, minimum, and mean values of the climate model are considered for the temporal disaggregation and are exactly reproduced in the sub-daily results. Thus, the Teddy-Tool allows for incorporating local sub-daily climate profiles and therefore reproducing seasonal and regional characteristics.

Then, we compare the levels of labour capacity based on daily and disaggregated hourly data. For this sensitivity analysis, we exemplarily selected RCP 7.0 of the UKESM1-0-LL climate model for 30 locations representing major global agricultural regions (see Fig. S11). Assuming a 7 a.m. to 7 p.m. workday, we find that, indeed, when using hourly data, the heat-induced labour losses could be substantially larger than when using the daily mean depending on latitude and season (see Fig. S12). The largest difference can be found in the summer seasons of continental climate zones (up to 30 percentage points), while tropical regions show lower and more uniform reductions throughout the year. However, we do not allow for shifts in the working hours, which could partly compensate heat-induced labour losses.

### Description of the production system in GRACE

Here, we description the production system for crops, which is implemented in GRACE. For irrigated crops, we adopt the structure of crop production similar to Luckmann et al. (2014) and

Orlov et al. (2021), which is illustrated in Fig. 1. Rainfed crops have the same production structure but without water as a production input. Sectoral production is modelled using nested constant elasticity of substitution (CES) functions. Adaptation in production is represented by substitution among production inputs (i.e., labour, capital, and land) as well as mobility of production inputs across sectors. Elasticities of substitution implemented in CES functions determine the degree of substitutability among production inputs. The substitution effect is determined by the value of substitution elasticity and the value share of production input.

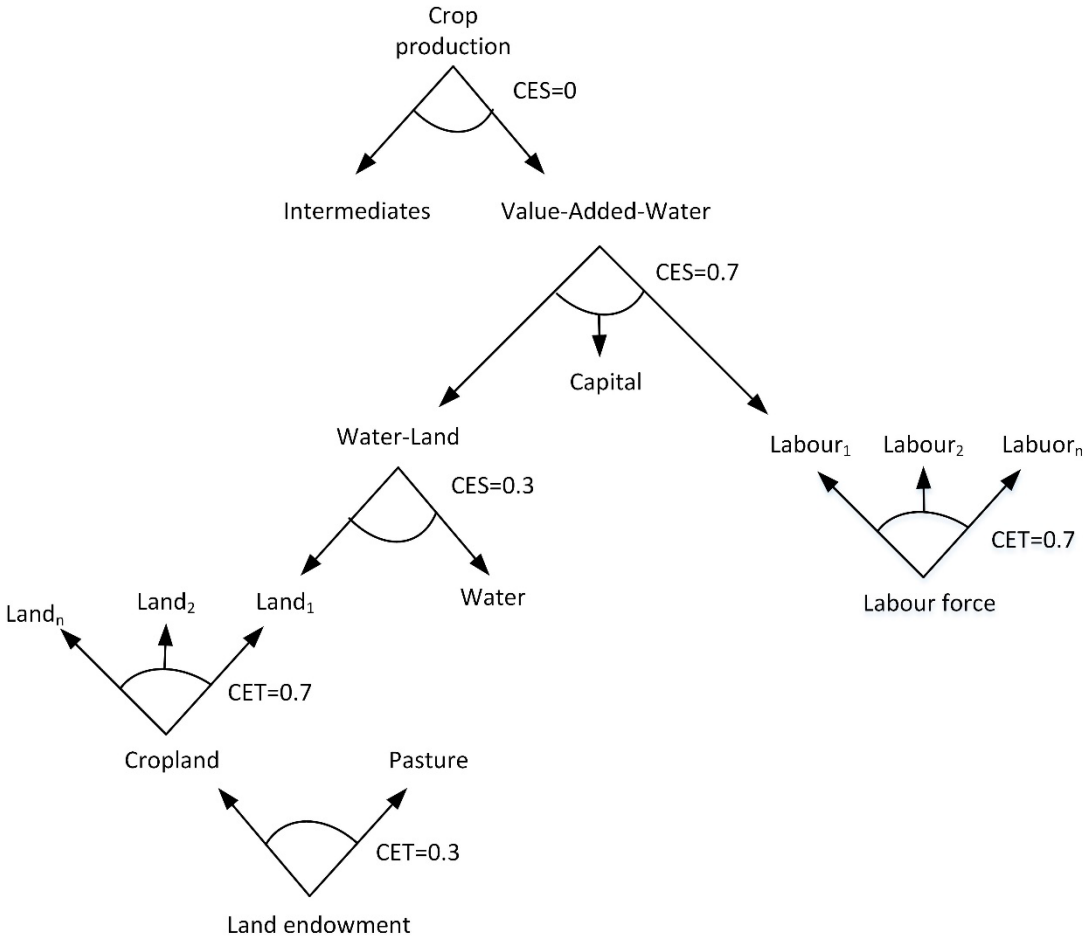


**Fig. 1:** Nested structure of production of irrigated crops.

At the top level of nested CES functions, production of crops is described by a Leontief production function over intermediates and the aggregate of value-added-water, which implies no substitutability between those two aggregates. At the second level, the aggregate of value-added-water ($VAW_i$) is a standard CES function over capital (see Eq. 1). In GRACE, equations are also region- and sector specific, and the indexes defining region and sector are removed from Eq. 1 for simplicity.

$$VAW = ad * \left[sh_f * WL^r + sh_f * C^r + sh_f * L^r\right]^{\frac{1}{r}} \quad \text{Eq. 1}$$

where

*VAW* is the value-added aggregate in a sector
*WL* is the aggregate of water-land in a sector
*C* is capital input in a sector
*L* is labour input in a sector
*ad* is the shifter parameter for CES function in a sector
*sh* is the factor-specific share parameter in a sector
*r* is the elasticity parameter, which equals to: $r = 1 - \frac{1}{\sigma}$
$\sigma$ is the substitution elasticity

The elasticity of substitution between capital, labour, and the aggregate of water-land, which measures the change in the ratio of inputs with respect to the ratio of their prices, is assumed to equal 0.7. The empirical literature rejects the hypothesis of a Cobb-Douglas function, which implies a substitution elasticity between capital and labour of one, and shows that the substitution elasticity tends to be less than one [4,5]. In GRACE, the default value of the substitution elasticity between capital, labour, and the aggregate of water-land is assumed to equal 0.7, which is supported by empirical evidence [6–8]. At the third level, the aggregate of water-land is depicted by a standard CES function over water and land. The substitution elasticity between water and land tends to have a small value ranking from 0 to 0.3 [2,9,10]. In our analysis, the value of this substitution elasticity is assumed to equal 0.3.

The allocation of land among sectors is modelled using a two-level nested constant elasticity of transformation (CET) function. At the first level, land is allocated between cropland and other sectors (e.g., pasture) using a CET function with a transformation elasticity of 0.3. At the second level, a CET function allocates cropland among different types of crops. In different CGE-based studies, the value of transformation elasticity for cropland among different types of crops varies from 0 to 1 [10–15]. In our analysis, the value of transformation elasticity for cropland is assumed to equal 0.7. Following Gaasland (2008), labour allocation is modelled to be imperfectly mobile across sectors using a constant elasticity of transformation (CET) function with a transformation elasticity of 3.

**Description of the price system in GRACE**

Equilibrium prices are determined by interactions of demand and supply. In CGE models, equilibrium in commodity and factor markets are achieved when three main conditions are satisfied, such as i) market clearance (i.e., demand should be equal supply), ii) zero profit (i.e., production revenues should be equal production costs), and iii) income balance (i.e.,

consumer's income should be equal expenditures). These conditions are achieved through market mechanisms and adjustments, such as mobility (re-allocation) production factors (i.e., labour, capital, and land) across sectors, substitution among production factors, changes in trade and consumption, and substitution in consumption of commodities.

Producer prices are determined by unit cost of production inputs, such as intermediates, labour, capital, and land. For example, the price formation of irrigated crops is shown in Fig. 2. The producer price of an irrigated crop (PD) is determined by an aggregate price of intermediates (PIO) and an aggregate price of value-added including water (PVAW). The price of value-added is determined by factor prices for capital, labour, and land ($PFA_{f,}$) and the price of water input ($P_{water}$). The consumer price of a crop (P) is determined by a domestic producer price (PD) and an import price of crop (PIM). GRACE is formulated as a mixed-complementarity problem (MCP) [17–19]. Commodity and factor prices are defined as the complementary variables to zero profit conditions for commodity and factor markets, while the aggregate prices, such as the price of value-added, is defined as unit cost functions derived from CES functions (Eq. 2). Note that in GRACE, equations are region- and sector specific, and the indexes defining region and sector are removed from Eq. 2 for simplicity.

$$PVAW = \frac{1}{ad} * \left[sh^{\sigma} * PWL^{1-\sigma} + sh_{capital}^{\sigma} * PFA_{capital}^{1-\sigma} + sh_{labour}^{\sigma} * PFA_{labour}^{1-\sigma}\right]^{\frac{1}{1-\sigma}}$$

Eq. 2

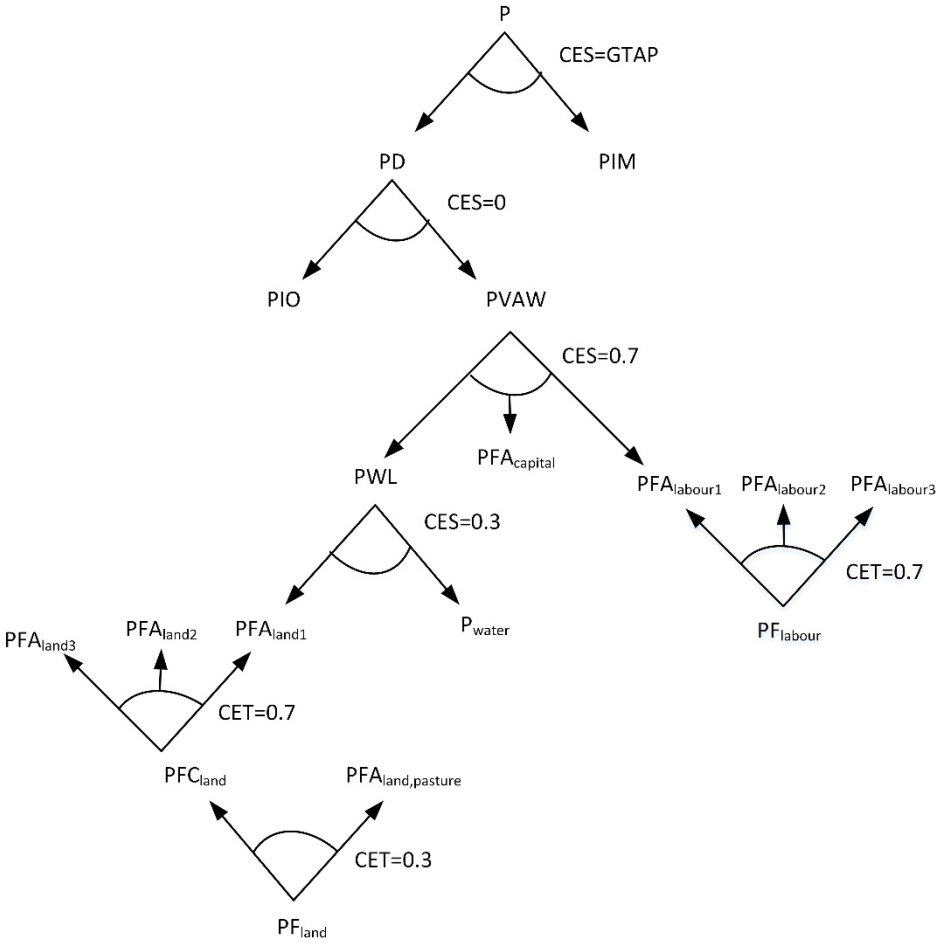


**Fig. 2:** Price system for irrigated crops.

A productivity shock affects the production cost (PD) and the returns to factors of production (i.e., wages and profit) ($PFA_f$). To minimise the cost, producers adjust their production through substitution of inputs as well as factor mobility. In response to changes in producer prices and income, consumers adjust their consumption by choosing how much and what to consume. Imported and domestically produced commodities are assumed to be imperfect substitutes, which is modelled using the Armington approach (i.e., CES functions). The elasticity of substitution between imported and domestic commodities are obtained from the GTAP database. Moreover, different commodities (e.g., different crops or food vs. non-food) are assumed to be imperfect substitutes in private consumption (i.e., substitution effect). Moreover, a demand response of staple crops is also determined by changes in relative prices of staple crops and other goods (i.e., food and non-food). For example, in rich countries, people would consume more "luxury" items if food becomes cheaper (i.e., income effect). Changes in commodity and factor prices lead to a new market equilibrium through re-allocation of production inputs across sectors, substitution effects, and changes in trade and consumption

patterns. Substitution effects in production and consumption of commodities induce non-linearity in economic responses.

**Formation of consumer prices**

In the GRACE model, the price response is determined by interactions between demand and supply, given the assumption of market equilibrium (i.e., demand equals supply) (Fig. 3). As the GRACE model explicitly depicts bilateral trade, the demand for commodities consists of domestic supply (minus export) and import. In the presence of trade, in addition to domestic production, the response of global supply of crops also determines the response of consumer prices. Similar to other CGE models, in GRACE, domestic and imported commodities are assumed to be imperfect substitutes and therefore, the price response differs by region, depending on the share of imported commodities in total consumption and the shock on crop productivity. The response of consumer prices and domestic production can be asymmetric because of trade possibility. For example, a region can experience a climate-induced reduction in production of crops and, at the same time, a reduction in the consumer price, if there is a global increase in production, leading to a higher import demand. However, if the yield shock is relatively strong and the domestic demand is mainly satisfied through the domestic supply, then a reduction in domestic production could lead to an increase in the regional consumer price of crops due to imperfect substitutability between domestically produced and imported crops.

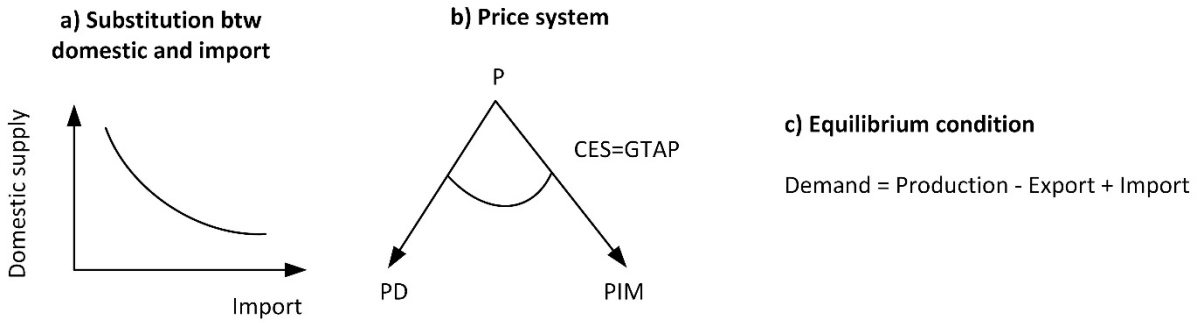


**Fig. 3:** Formation of consumer prices.

## Supplementary Tables

**Table S1:** Regional aggregation.

| **Regions** | **Countries** |
|---|---|
| W-Europe (Western Europe) | Albania, Austria, Belgium, Switzerland, Germany, Denmark, Spain, Estonia, Finland, France, United Kingdom, Greece, Croatia, Ireland, Italy, Lithuania, Luxembourg, Latvia, Netherlands, Norway, Portugal, Slovenia, Sweden |
| W-Asia (Western Asia) | United Arab Emirates, Armenia, Azerbaijan, Cyprus, Georgia, Israel, Jordan, Kuwait, Oman, Qatar, Saudi Arabia, Turkey, Iraq, Lebanon, Syria, Yemen |
| L-America (Latin America) | Argentina, Bolivia, Brazil, Chile, Colombia, Costa Rica, Dominican Republic, Ecuador, Guatemala, Honduras, Jamaica, Mexico, Nicaragua, Panama, Peru, Puerto Rico, Paraguay, El Salvador, Trinidad & Tobago, Uruguay, Venezuela |
| Oceania | Australia, New Zealand |
| Africa | Benin, Burkina Faso, Botswana, Côte d'Ivoire, Cameroon, Egypt, Ethiopia, Ghana, Kenya, Morocco, Madagascar, Mozambique, Mauritius, Malawi, Namibia, Nigeria, Rwanda, Senegal, Togo, Tunisia, Tanzania, Uganda, Angola, Congo - Kinshasa, Chad, Congo - Brazzaville, Equatorial Guinea, Gabon, São Tomé & Príncipe, Central African Republic, Burundi, Comoros, Djibouti, Eritrea, Mayotte, Seychelles, Somalia, Sudan, South Sudan, Algeria, Libya, Cape Verde, Gambia, Guinea-Bissau, Mali, Mauritania, Niger, St. Helena, Sierra Leone, South Africa, Zambia, Zimbabwe |
| S-Asia (Southern Asia) | Bangladesh, India, Iran, Sri Lanka, Nepal, Pakistan, Afghanistan, Bhutan, Maldives |
| E-Europe (Russia and Eastern Europe) | Bulgaria, Belarus, Czechia, Hungary, Poland, Romania, Russia, Slovakia, Ukraine |
| SE-Asia (South-East Asia) | Brunei, Indonesia, Cambodia, Laos, Malaysia, Philippines, Thailand, Vietnam, Myanmar (Burma) |
| N-America (North America) | Canada, United States |
| E-Asia (East Asia) | China, Hong Kong SAR China, Japan, South Korea, Mongolia, Taiwan |
| C-Asia (Central Asia) | Kazakhstan, Kyrgyzstan, Tajikistan, Turkmenistan, Uzbekistan |

## Supplementary Figures

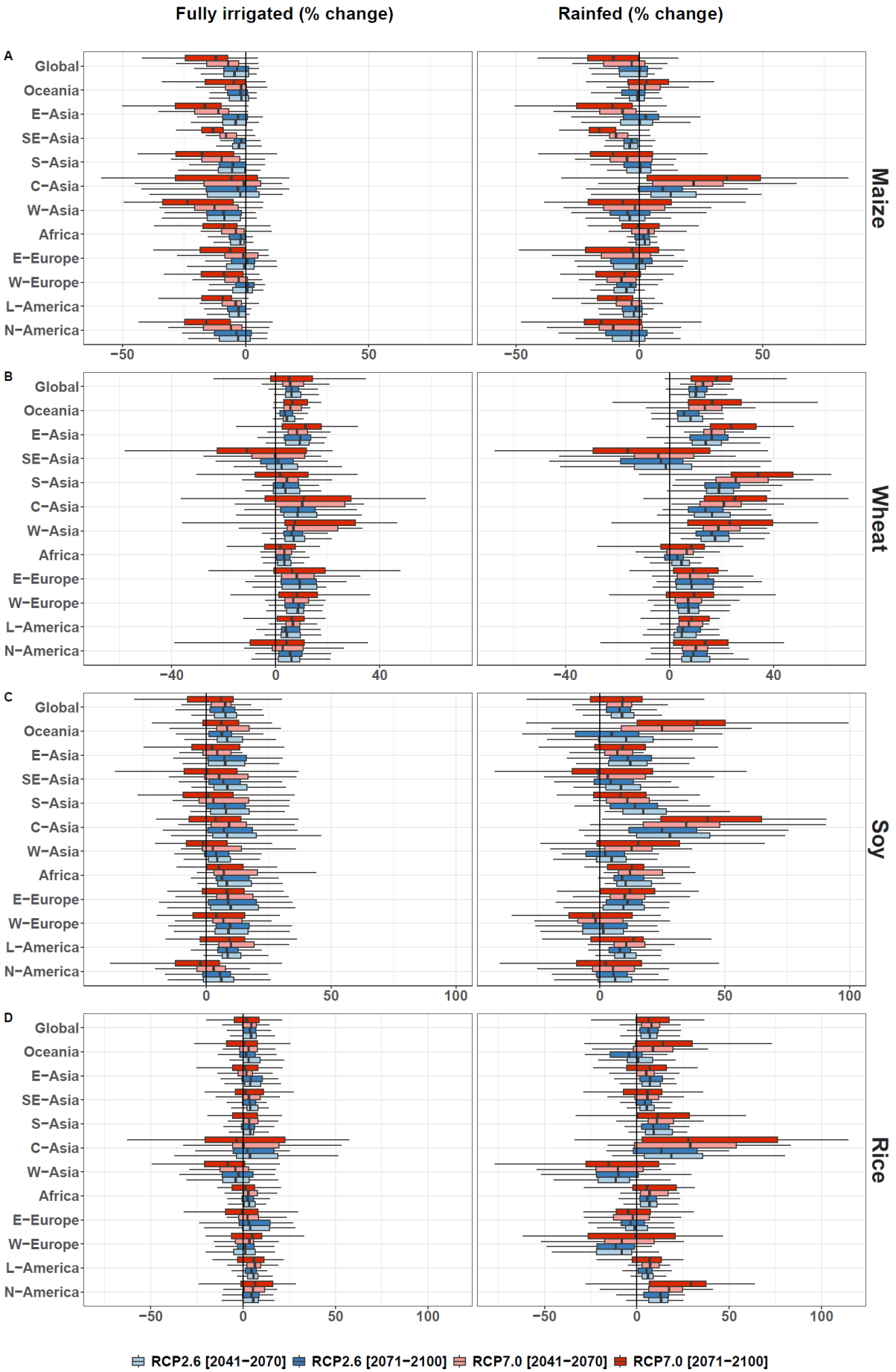
Fully irrigated (% change)
Rainfed (% change)
A
B
C
D
Global
Oceania
E−Asia
SE−Asia
S−Asia
C−Asia
W−Asia
Africa
E−Europe
W−Europe
L−America
N−America
Maize
Wheat
Soy
Rice
−50
0
50
−40
40
100
RCP2.6 [2041−2070]
RCP2.6 [2071−2100]
RCP7.0 [2041−2070]
RCP7.0 [2071−2100]

**Fig. S1:** Multi-year mean changes in regional harvested-area-weighted yields of fully irrigated and rainfed maize (A), wheat (B), soy (C), and rice (D) by the mid [2041–2070] and end [2071–2100] of the century under RCP2.6 (blue) and RCP7.0 (red) relative to the average yield in the historical time period [1981-2010]. The boxes show the interquartile range across climate and crop model ensembles. The whiskers show the variability outside the 1st and 3rd quantiles, and outliers are removed.

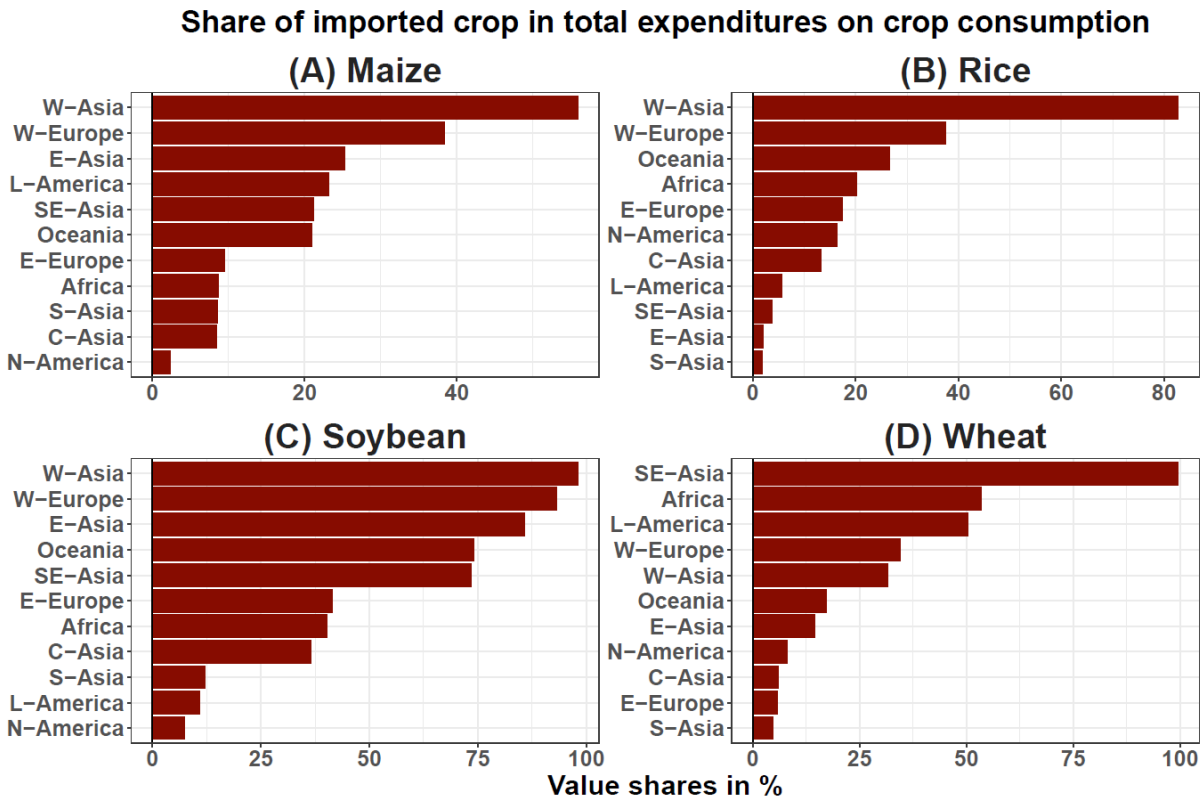


**Fig. S2:** Shares of imported maize (A), rice (B), soybean (C), and wheat (D) in total expenditures on imported and domestically produced crops (in percent). Own calculations based on version 9 of the GTAP database for 2011 reference period.

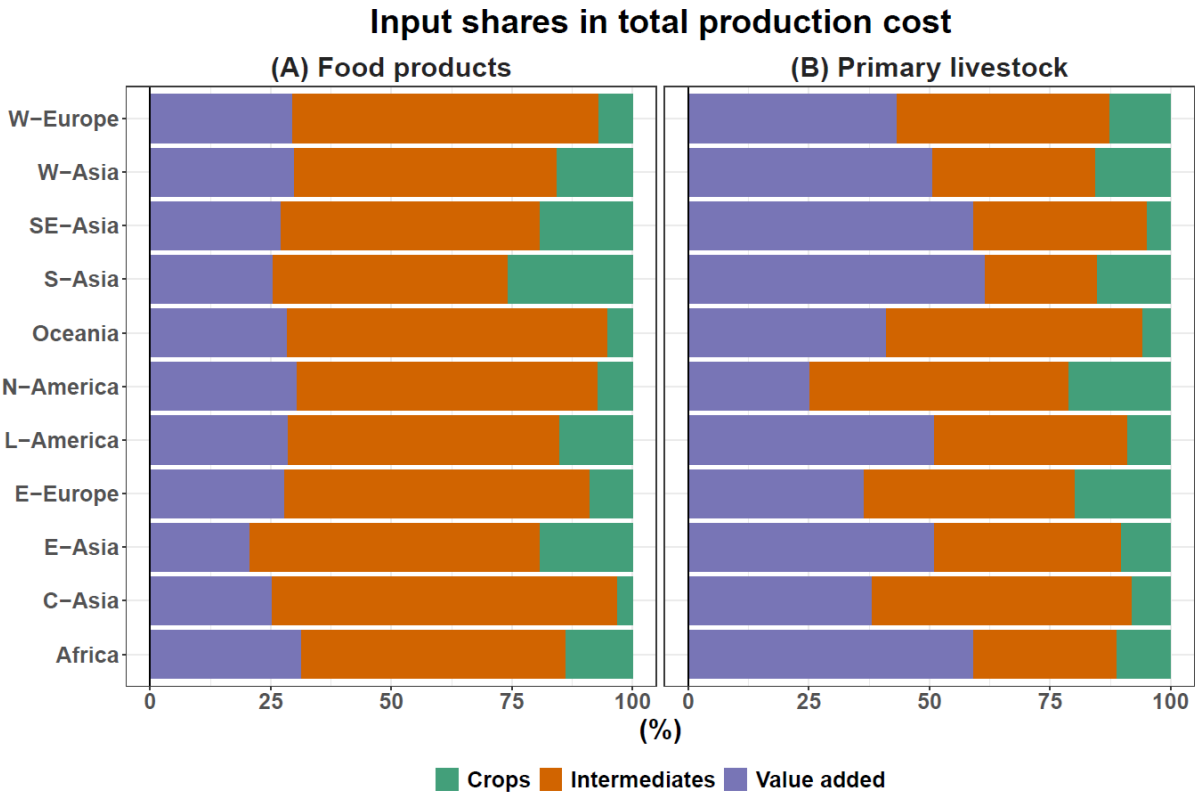


**Fig. S3:** Shares of crops, intermediates, and value added in total production cost of food products (A) and primary livestock (B) (in percent). Own calculations based on version 9 of the GTAP database for 2011 reference period.

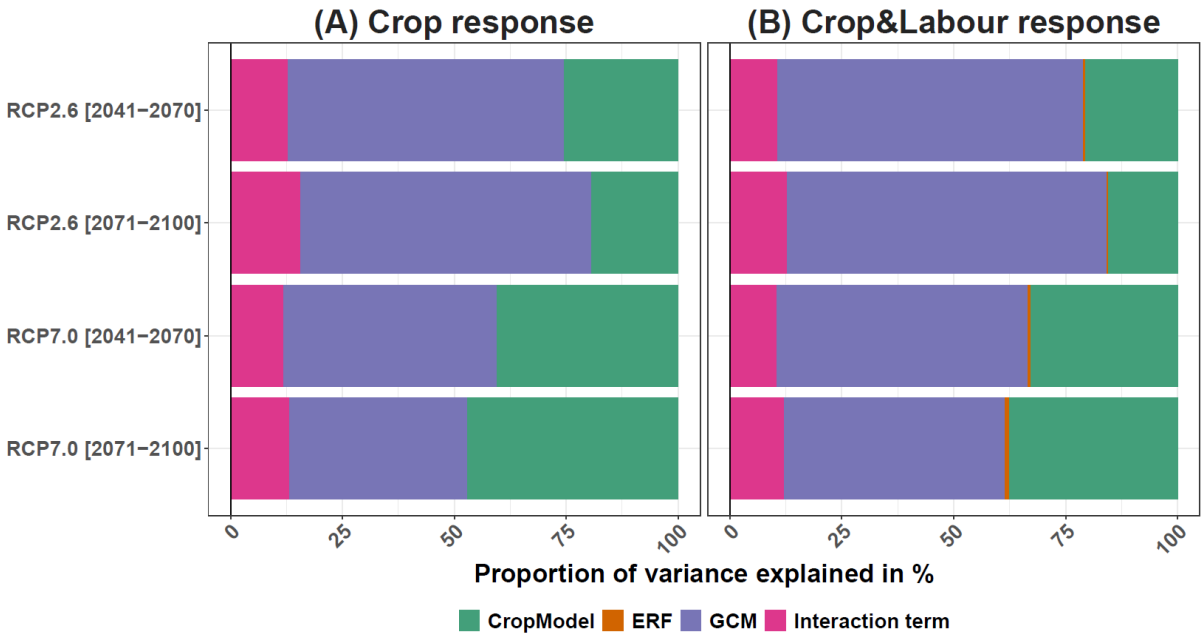


**Fig. S4**: Analysis of variance for global real income. The legend "GCM" stands for the GCM-related uncertainty, "CropModel" is for the uncertainty of crop model simulations "ERF" is for the uncertainty of heat-labour exposure response functions. "Crop response" (A) show the scenarios that only consider the climate-related yield responses of the four crops. The triangles in shades of orange labelled "Crop&Labour response" (B) show the scenarios that consider both yield changes and heat stress impacts on labour of the four crops.

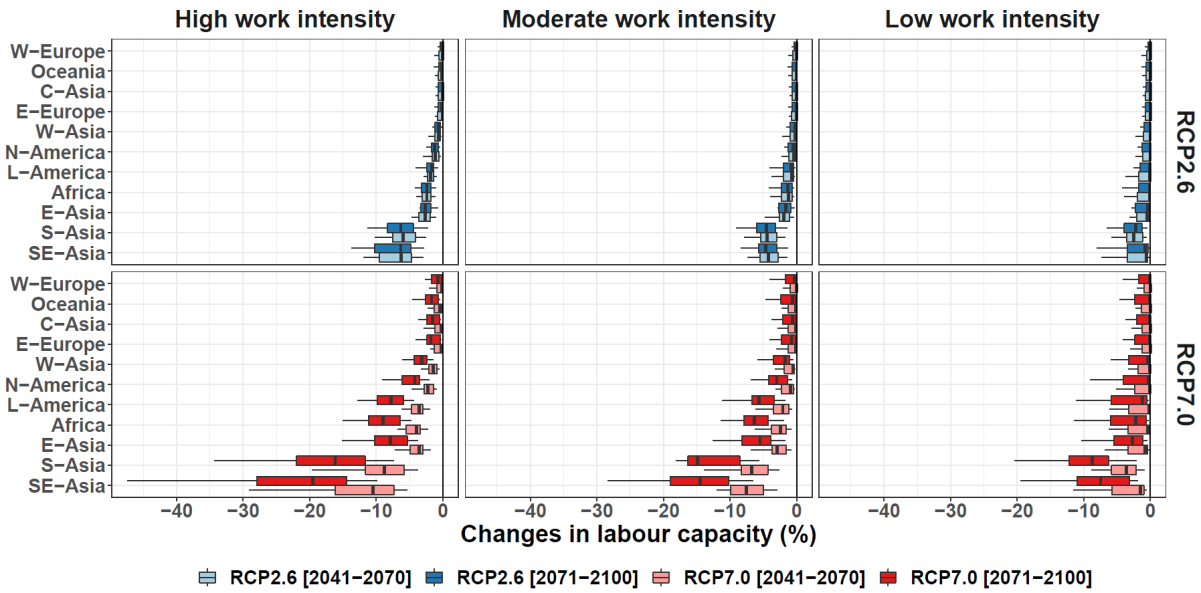


**Fig. S5:** Area-weighted multi-year mean changes in labour capacity in production of all crops by the mid [2041–2070] and end [2071–2100] of the century under RCP2.6 (blue) and RCP7.0 (red) relative to the average yield in the historical time period [1981–2010]. The boxes show the interquartile range across climate models ensemble and labour-heat exposure-response functions. The whiskers show the variability outside the 1st and 3rd quantiles. The dots show outliers.

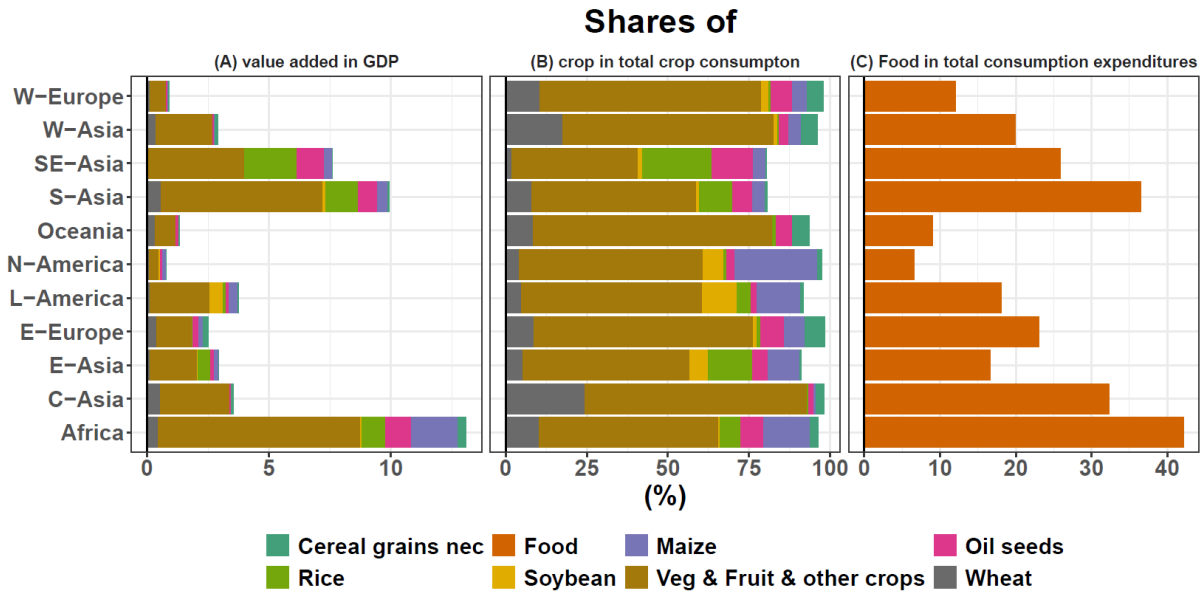


**Fig. S6:** Shares of value added in GDP (A), shares of crops in total expenditures on crop consumption (B), and shares of food in total consumption expenditures (C) (in percent). Own calculations based on version 9 of the GTAP database for 2011 reference period.

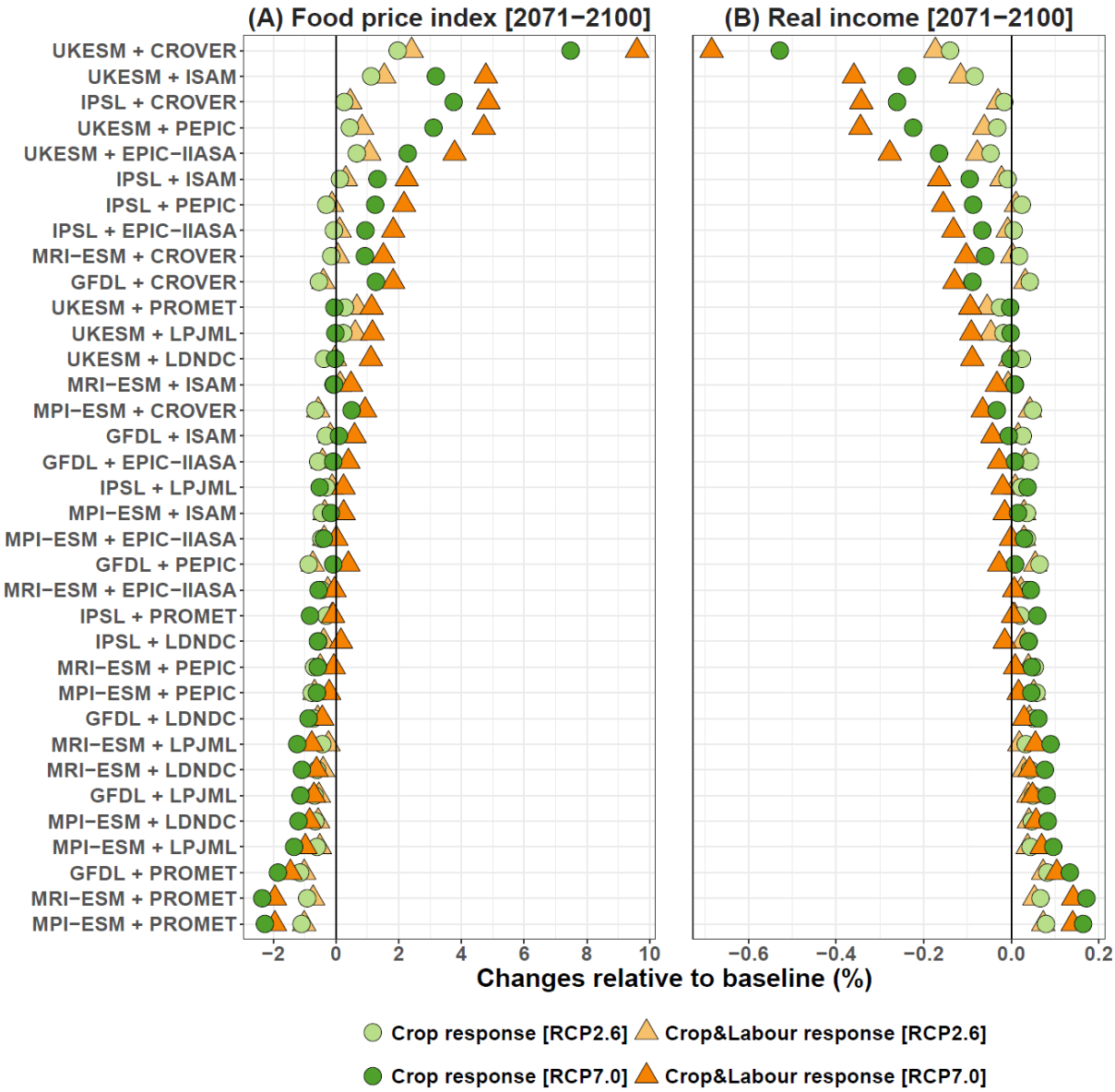


**Fig. S7:** Median responses of global food price index (A) and real income (B) by the end [2071–2100] of the century under RCP2.6 and RCP7.0 for each climate and crop model combination relative to the historical time period. The income and price responses are simulated using GRACE and show the median changes over GCMs, crop models, and exposure-response functions relative to the state of the world economy in 2011. The circles in shades of green labelled "Crop response" show the scenarios that only consider the climate-related yield responses of the four crops. The triangles in shades of orange labelled "Crop&Labour response" show the scenarios that consider both yield changes and heat stress impacts on labour of the four crops.

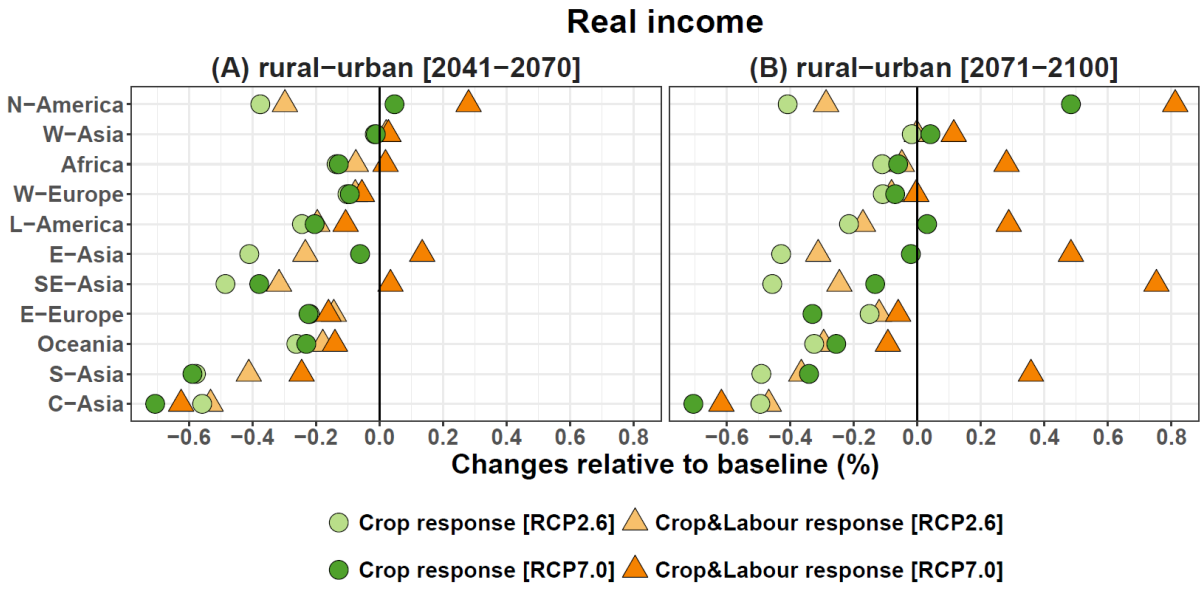


**Fig. S8:** Median responses of changes in the rural-urban income ratio by the mid [2040–2070] (A) and end [2071–2100] (B) of the century under RCP2.6 and RCP7.0 relative to the historical time period. The income responses are simulated using the GRACE model and show the median changes over GCMs, and crop models, and exposure-response functions relative to the state of the world economy in 2011. The circles in shades of green labelled "Crop response" show the scenarios that only consider the climate-related yield responses of the four crops. The triangles in shades of orange labelled "Crop&Labour response" show the scenarios that consider both yield changes and heat stress impacts on labour of the four crops. A positive (negative) number means that a decrease (increase) in income gap between rural and urban households.

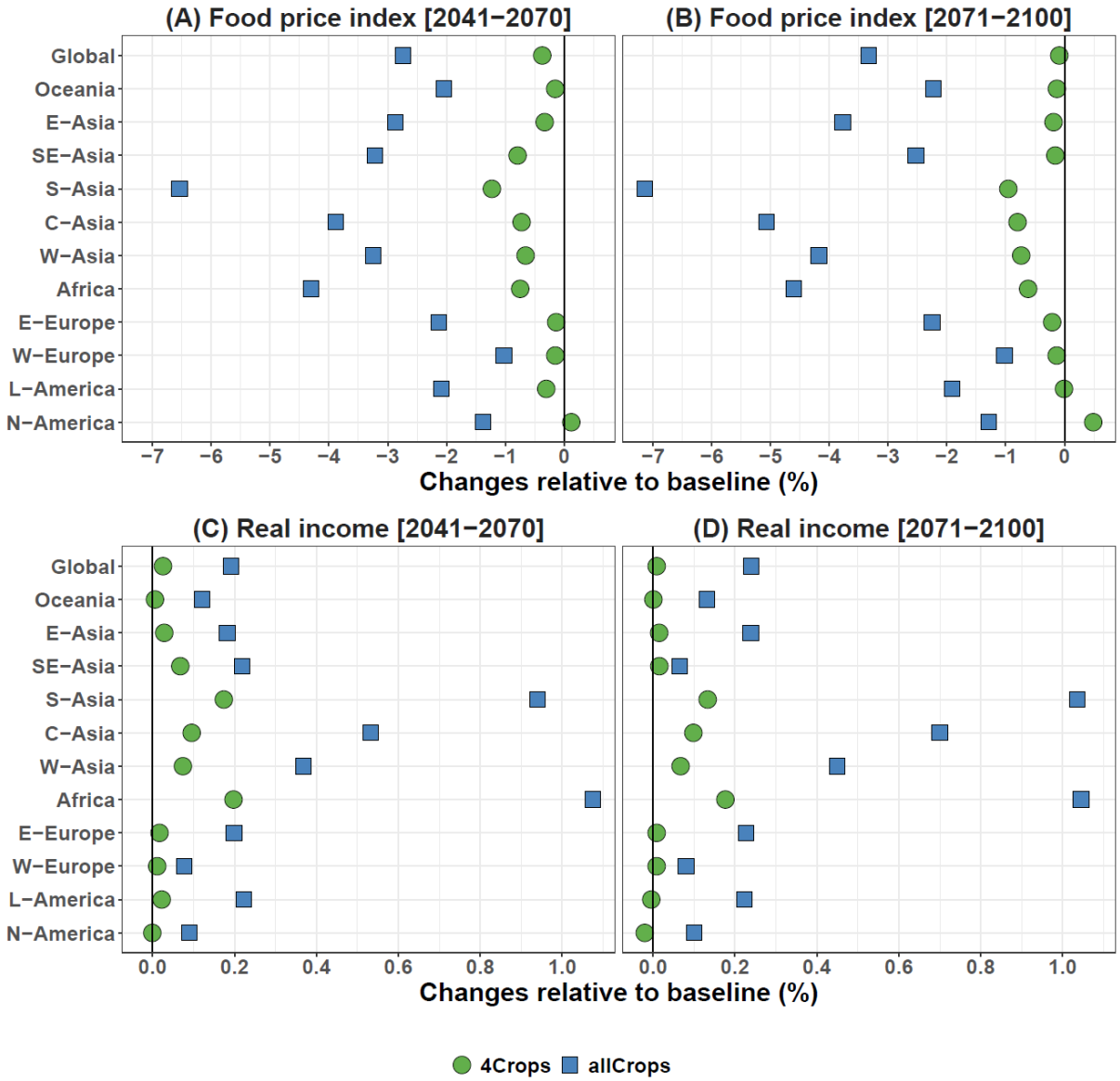


**Fig. S9:** Median responses of the food price index by the mid [2041–2070] (A) and end [2071–2100] (B) of the century, and regional real income by the mid [2041–2070] (C) and end [2071–2100] (D) of the century under RCP7.0 relative to the historical time period. The income responses are simulated using the GRACE model and show the median changes over GCMs and crop models relative to the state of the world economy in 2011. Heat stress impacts on labour are not included. The green circles show the scenarios that only consider the climate-related yield responses of for major crops. The blue squares show the scenario that consider the climate-related yield responses of all types of crops.

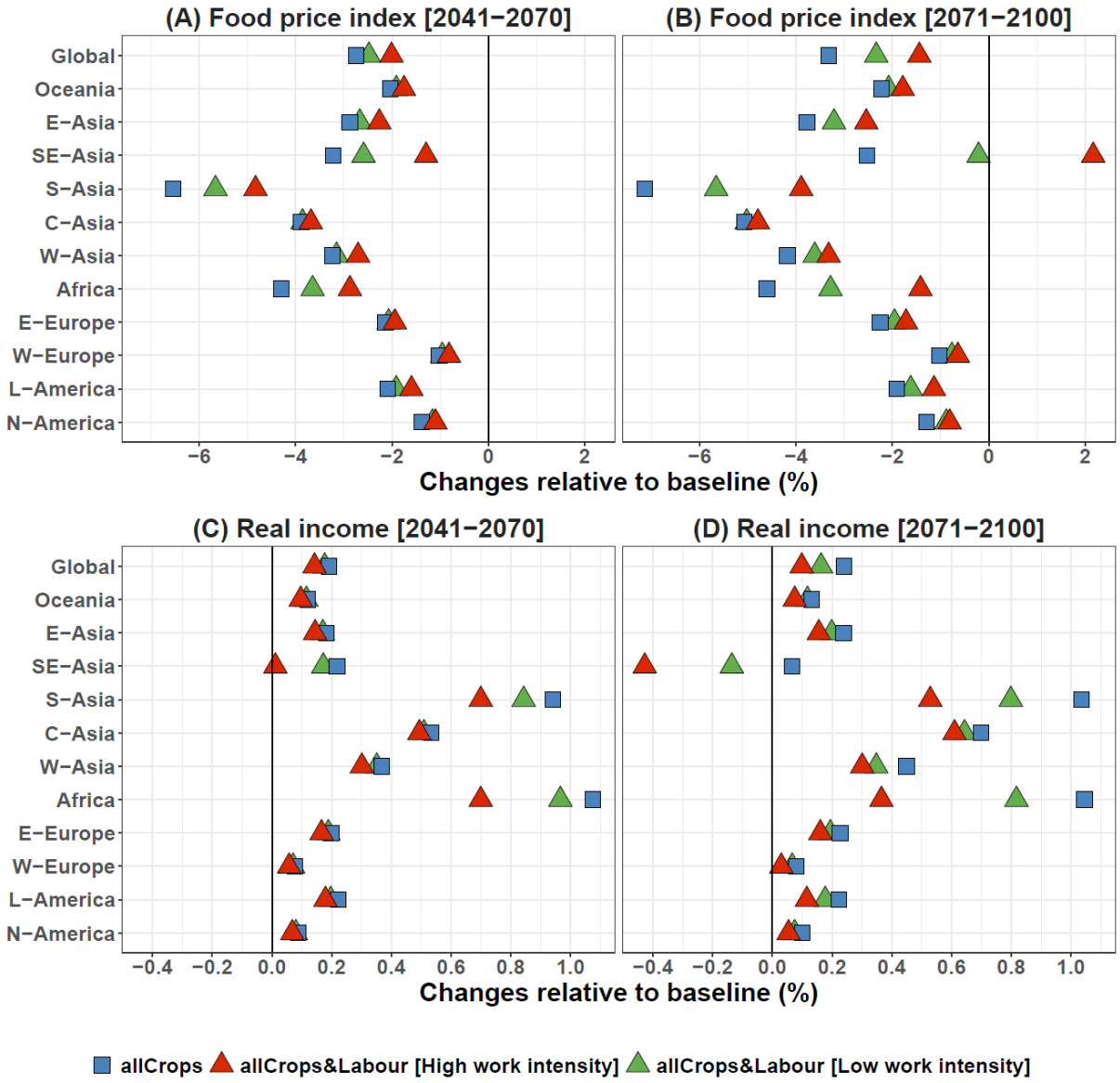


**Fig. S10:** Median responses of the food price index by the mid [2041–2070] (A) and end [2071–2100] (B) of the century, and regional real income by the mid [2041–2070] (C) and end [2071–2100] (D) of the century under RCP7.0 relative to the historical time period. The income responses are simulated using the GRACE model and show the median changes over GCMs, crop models, and heat-labour exposure-response functions relative to the state of the world economy in 2011. The blue squares show the scenarios that only consider the climate-related yield responses of all types of crops. The red triangles show the scenario that consider both yield changes and heat stress impacts on labour with high work intensity. The orange triangles are the same as the former but with a radical mechanisation deployment in crop production.

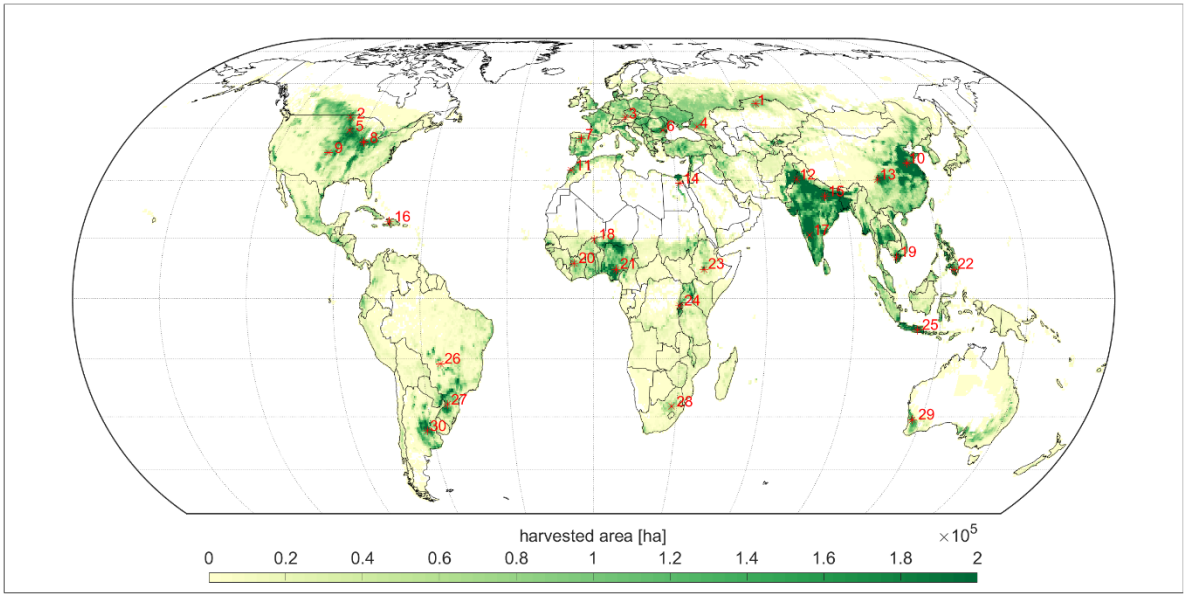


**Fig. S11:** Sample members selected to compare the levels of labour capacity which are calculated using hourly and daily mean climate data.

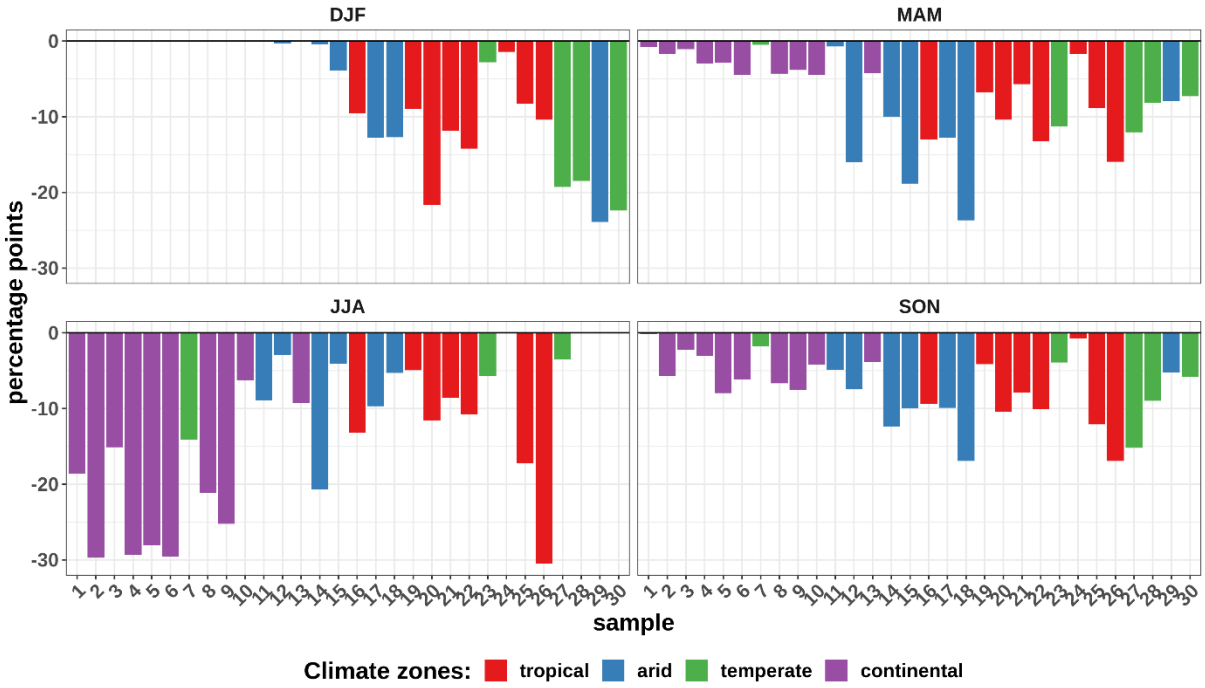


**Fig. S12:** Absolute differences between the levels of labour capacity calculated using hourly climate data for a 7 a.m. to 7 p.m. workday and those calculated using daily mean values of UKESM1-0-LL by the end of the century [2071–2100] under RCP7.0. The X-axis indicates the sample members (Fig. S11), which are ordered by latitude. Negative values show that when using hourly climate data, the labour capacity is smaller compared to when daily mean values of climate data are used. Labour capacity is estimated using the NIOSH exposure-response functions.

## Supplemental References:


1. Zabel, F., and Poschlod, B. (2023). The Teddy tool v1.1: temporal disaggregation of daily climate model data for climate impact analysis. Geosci. Model Dev. *16*, 5383–5399. https://doi.org/10.5194/gmd-16-5383-2023.

2. Luckmann, J., Grethe, H., McDonald, S., Orlov, A., and Siddig, K. (2014). An integrated economic model of multiple types and uses of water. Water Resour. Res. *50*, 3875–3892. https://doi.org/10.1002/2013WR014750.

3. Orlov, A., Daloz, A.S., Sillmann, J., Thiery, W., Douzal, C., Lejeune, Q., and Schleussner, C. (2021). Global Economic Responses to Heat Stress Impacts on Worker Productivity in Crop Production. Econ. Disasters Clim. Change. https://doi.org/10.1007/s41885-021-00091-6.

4. Arrow, K.J., Chenery, H.B., Minhas, B.S., and Solow, R.M. (1961). Capital-Labor Substitution and Economic Efficiency. Rev. Econ. Stat. *43*, 225–250. https://doi.org/10.2307/1927286.

5. Gechert, S., Havranek, T., Irsova, Z., and Kolcunova, D. (2022). Measuring capital-labor substitution: The importance of method choices and publication bias. Rev. Econ. Dyn. *45*, 55–82. https://doi.org/10.1016/j.red.2021.05.003.

6. Antoszewski, M. (2019). Wide-range estimation of various substitution elasticities for CES production functions at the sectoral level. Energy Econ. *83*, 272–289. https://doi.org/10.1016/j.eneco.2019.07.016.

7. Knoblach, M., Roessler, M., and Zwerschke, P. (2020). The Elasticity of Substitution Between Capital and Labour in the US Economy: A Meta-Regression Analysis. Oxf. Bull. Econ. Stat. *82*, 62–82. https://doi.org/10.1111/obes.12312.

8. Mućk, J. (2017). Elasticity of substitution between labor and capital: robust evidence from developed economies. NBP Work. Pap.

9. Calzadilla, A., Rehdanz, K., and Tol, R.S.J. (2011). The GTAP-W model: Accounting for water use in agriculture (Kiel Institute for the World Economy (IfW)).

10. Philip, J.-M., Sánchez-Chóliz, J., and Sarasa, C. (2014). Technological change in irrigated agriculture in a semiarid region of Spain. Water Resour. Res. *50*, 9221–9235. https://doi.org/10.1002/2014WR015728.

11. Hertel, T., and Liu, J. (2019). Implications of Water Scarcity for Economic Growth. In Economy-Wide Modeling of Water at Regional and Global Scales Advances in Applied General Equilibrium Modeling., G. Wittwer, ed. (Springer), pp. 11–35. https://doi.org/10.1007/978-981-13-6101-2_2.

12. Hertel, T.W., Golub, A.A., Jones, A.D., O'Hare, M., Plevin, R.J., and Kammen, D.M. (2010). Effects of US Maize Ethanol on Global Land Use and Greenhouse Gas Emissions: Estimating Market-mediated Responses. BioScience *60*, 223–231. https://doi.org/10.1525/bio.2010.60.3.8.

13. Keeney, R., and Hertel, T.W. (2009). The Indirect Land Use Impacts of United States Biofuel Policies: The Importance of Acreage, Yield, and Bilateral Trade Responses. Am. J. Agric. Econ. *91*, 895–909.

14. Palatnik, R.R., Eboli, F., Ghermandi, A., Kan, I., Rapaport-Rom, M., and Shechter, M. (2011). Integration of general and partial equilibrium agricultural land-use transformation for the analysis of climate change in the mediterranean. Clim. Change Econ. *02*, 275–299. https://doi.org/10.1142/S2010007811000310.

15. Zhao, X., van der Mensbrugghe, D.Y., Keeney, R.M., and Tyner, W.E. (2019). Improving the way land use change is handled in economic models. Econ. Model. https://doi.org/10.1016/j.econmod.2019.03.003.

16. Gaasland, I. (2008). Modelling farmers' labour supply in CGE models (SNF).

17. Aaheim, H.A., Orlov, A., Wei, T., and Glomsrød, S. (2018). GRACE model and applications. CICERO Center for International Climate Research. Oslo, Norway. CICERO Reports; 2018:01. p. 1-45.

18. Mathiesen, L. (1985). Computation of economic equilibria by a sequence of linear complementarity problems. In Economic Equilibrium: Model Formulation and Solution Mathematical Programming Studies., A. S. Manne, ed. (Springer), pp. 144–162. https://doi.org/10.1007/BFb0121030.

19. Rutherford, T.F. (1995). Extension of GAMS for complementarity problems arising in applied economic analysis. J. Econ. Dyn. Control *19*, 1299–1324. https://doi.org/10.1016/0165-1889(94)00831-2.